Nanoscale

Accepted Manuscript

This article can be cited before page numbers have been issued, to do this please use: Z. Chen, Y. Xie, W. Huang, C. Qin, A. Yu and G. Lai, *Nanoscale*, 2019, DOI: 10.1039/C9NR02543J.

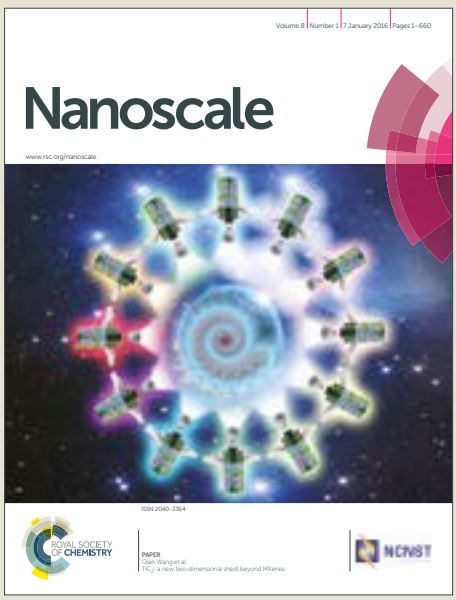

ROYAL SOCIETY OF CHEMISTRY

rsc.li/nanoscale

Exonuclease-assisted target recycling for ultrasensitive electrochemical detection of microRNA at vertically aligned carbon nanotubes†

Zhichao Chen,[a] Yiming Xie,[a] Wan Huang,[a] Chuanying Qin,[a] Aimin Yu,[a,b] Guosong Lai*[a]

[a] *Hubei Key Laboratory of Pollutant Analysis & Reuse Technology, Department of Chemistry, Hubei Normal University, Huangshi 435002, PR China*

[b] *Department of Chemistry and Biotechnology, Faculty of Science, Engineering and Technology, Swinburne University of Technology, Hawthorn VIC 3122, Australia*

*Corresponding author

E-mail address: gslai@hbnu.edu.cn (G. Lai).

†Electronic supplementary information (ESI) available. See DOI: 10.1039/******

Abstract: As an important biomarker for early disease diagnosis, microRNA-21 (miRNA-21) has attracted considerable attentions concerning its accurate detection. Herein we combine the one-step biorecognition reaction at a vertically aligned nanostructure-based biosensor with the T7 exonuclease (Exo)-assisted target recycling to develop a novel electrochemical bioassay method for miRNA-21 detection. The vertically aligned nanointerface is constructed through the covalent attachment of terminally carboxylated single-walled carbon nanotube (SWCNT) at an aryldiazonium salt-modified electrode, which enables the noncovalent adsorption of ferrocene (Fc)-labeled single-stranded signal DNA to obtain the biosensor. Upon its incubation with a target miRNA-21 solution, the DNA/RNA hybridized duplexes will form and release from the electrode surface, leading to corresponding electrochemical signal decrease of the biosensor. Moreover, this biorecognition reaction can also trigger the T7 Exo-assisted target recycling to achieve the great signal amplification. Together with the highly efficient biorecognition and excellent electron transfer promotion at the vertically aligned SWCNTs, this biosensor exhibits a wide linear range varying from 0.01 to 100 pM and a low detection limit down to 3.5 fM. Considering its obvious performance superiority and convenient manipulations, this vertically aligned SWCNT-based electrochemical biosensing method has extensive potentials for practical applications.

Keywords: Biosensor; Carbon nanomaterials; Electroanalytical chemistry; microRNA assay; Exonuclease

1. Introduction

As a class of noncoding RNA molecules with a length of approximately 18–24 nucleotides, microRNAs (miRNAs) have been demonstrated to be important biomarkers for the clinical diagnosis of a wide variety of deseases.[1,2] Thus, the development of useful methods for the sensitive and selective detection of miRNA in complicated physiological matrices is of great importance. In comparison with the conventional biological methods, the biosensors which are constructed on basis of the highly specific nucleic acid hybridizations have shown powerful ability on this issue due to their outstanding advantages such as high selectivity, small sample consumption and relatively low analytical cost.[3–5]

During the biosensing process, the most important thing is to develop effective strategies to achieve sensitive and convenient signal transduction. So far, various analytical approaches such as electrochemistry,[6,7] colorimetry,[8,9] fluorescence,[10,11] electrochemiluminescence[12,13] and photoelectrochemical methods[14,15] have been extensively employed for the miRNA biosensor construction. Among them, various nanomaterial-modified electrodes are often the popular choices in the development of different ultrasensitive electrochemical biosensing strategies to fulfil the accurate detection of low-abundant miRNAs in the early disease diagnosis field.[16–19] On one side, the nanomaterials with large specific area and high electroconductivity can be used for the electrode modification in order to enhance the immobilization of the biorecognition agents and accelerate the electron transfer of biosensors.[20,21] However, how to control the orientation of the nanomaterial modification on the electrode surface and thus improve the biorecognition efficiency and decrease the nonspecific adsorption is still a great challenge. On the other hand, various nanoprobes prepared from the high loading of different signal labels on nanomaterials are often used for the signal transduction of biosensors.[22–24]

View Article Online
DOI: 10.1039/C9NR02543J

Although the mulitiple label signal amplification of these nanoprobes can drastically enhance the sensitivity, the complicated nanoprobe synthesis and their quantitative capture for heterogeneous bioassays not only require a relatively long time and specialized operations but also take unavailable effects to the repeatability of the methods.

As a carbon nanomaterials possessing extraordinary mechanical, electronic and optical properties, single-walled carbon nanotubes (SWCNTs) have exhibited their versatile applications in the electrochemical biosensing field.[25] Besides their large specific surface area, high electroconductivity and easy functionalization, the low dimensional single-layer sp^2-hybridized carbon structures of SWCNTs decide their easy noncovalent adsorption of single-stranded nucleic acids through the π-π stacking interaction.[26] More importantly, the terminal activation of SWCNTs may realize their oriented assembly onto electrode surfaces to form vertically aligned nanostructures.[27,28] So this kind of aligned SWCNTs can act as useful molecular wires to fasten the heterogeneous electron transfer between the underlying electrodes and outside environments.[29] Meanwhile, the structural alignment of SWCNTs can also allow the complete exposure of their pristine sidewalls and thus improve the noncovalent adsorption of single-stranded nucleic acids and the biorecognition efficiency of the SWCNT-based biosensor greatly.[28]

Recently, the nuclease-based signal amplification techniques have gained considerable attentions in the bioassay and biosensing fields.[30] By using a variety of endonucleases, exonucleases, and nucleases, various target recycling strategies can be designed for the extreme increase of biosensing signal responses. Furthermore, in combination with various biorecognition reactions, a large variety of homogeneous bioassay approaches can be easily developed to avoid the complicated manipulations involving in the conventional heterogeneous biosensing methods.[31–33] Although several nuclease-based miRNA biosensing methods have been reported previously,[34–36] the complicated DNA primers and

View Article Online
DOI: 10.1039/C9NR02543J

enzymatic reactions involved in these systems unavoidably bring some restrictions to their analytical performance.

Hence, this work combines the one-step biorecognition reaction at a vertically aligned SWCNT-based biosensor and the T7 exonuclease (Exo)-assisted target recycling to develop a novel electrochemical biosensing method for the convenient and ultrasensitive detection of the model microRNA analyte of microRNA-21 (miRNA-21). As illustrated in Fig. 1, the vertically aligned nanostructures constructed through the covalent linking of the terminally carboxylated SWCNTs at an aryldiazonium-modified electrode provide an ideal platform for the noncovalent adsorption of the ferrocene-labeled single-stranded signal DNA (Fc-DNA) to obtain the biosensor. As the biorecognition reaction of miRNA-21 at the biosensor results in the formation of a DNA/RNA duplex, the Fc-DNA will release from the biosensor surface to cause corresponding electrochemical signal decrease. Moreover, this biorecognition reaction can also trigger the T7 Exo-assisted target recycling to amplify the signal decrease greatly. It thus achieves the ultrahigh electrochemical signal transduction of the biosensor for miRNA-21 bioassay.

Preferred position for Fig. 1

2. Experimental section

2.1 Reagents and materials.

Sodium nitrite, sodium perchlorate, *p*-phenylenediamine (PPD), 4-aminobenzoic acid (PABA) and 1-amino-3,6,9-trioxaundecanyl-11-ol (oligo-PEG) were purchased from Aladdin Co., Ltd (Shanghai, China). 1-(3-Dimethylaminopropyl)-3-ethylcarbodiimide hydrochloride (EDC) and N-hydroxy succinimide (NHS) were purchased from Sigma-Aldrich Co., Ltd. The high purified SWCNTs with the diameter of 1-2 nm and length of 1-3 μm were purchased from Xianfeng Nano Materials Co., Ltd (Nanjing, China). T7 Exo at the concentration of 100 U/μL in 50 mM pH 8.0 Tris-Ac containing 10

mM $MgCl_2$ was obtained from New England Biolabs Co. Ltd (Beijing, China). Ultrapure water with a resistivity of 18 MΩ cm was used in whole experiments. All oligonucleotides were synthesized by Sangon Biotechnology Co., Ltd (Shanghai, China), and their base sequences are listed as follows:

(1) Fc-DNA: 5'-Fc-TCA ACA TCA GTC TGA TAA-3';

(2) miRNA-21: 5'-UAG CUU AUC AGA CUG AUG UUG A-3';

(3) miRNA-155: 5'-UUA AUG CUA AUC GUG AUA GGG GU-3';

(4) miRNA-141: 5'-UAA CAC UGU CUG GUA AAG AUG G -3';

(5) miRNA-199a: 5'-ACA GUA GUC UGC ACA UUG GUU A -3'.

2.2 Apparatus

All electrochemical experiments such as cyclic voltammetry (CV), differential pulse voltammetry (DPV) and electrochemical impedance spectroscopy (EIS) were conducted at a CHI 660E electrochemical workstation (Chenhua, China). During the electrochemical measurements, an Ag/AgCl (3 M KCl) reference electrode, a platinum wire as the auxiliary electrode and a bare or modified gold electrode (2 mm in diameter) as the working electrode were used for the constitution of the three-electrode system. The atomic force microscopy (AFM) images were obtained with an Asylum Research MFP-3D™ atomic force microscope. The X-ray photoelectron spectroscopy (XPS) characterizations were performed with an Escalab 250Xi X-ray photoelectron spectrometer (Thermo Scientific).

2.3 Preparation of terminally carboxylated SWCNTs

First, 10 mg of SWCNTs were added into 100 mL of 4 M nitric acid and heated to 80 ^{o}C under magnetic stirring.[27] After conducting a refluxing reaction for 12 h, the products were centrifugated repeatedly and washed by water until to neutral condition. The obtained SWCNTs with terminal carboxyl groups were then transferred into a vacuum

View Article Online
DOI: 10.1039/C9NR02543J

oven and dried at room temperature for 12 h. Next, 5 mg of the above SWCNTs was added into 5 mL of a mixture of concentrated sulfuric and nitric acid (3:1), and then subjected to sonication for 8 h in an ice/water bath.[28] Follow that, the contents were poured into 100 mL water and left to settle overnight. After removing the supernatant, the obtained product was filtered with a 0.45 μm Millipore filter under suction. Finally, the dispersion permeated through the filtration membrane was centrifugated repeatedly and washed by water until pH was about pH 7.0. This leads to the successful collection of the chemically shortened SWCNTs with terminal carboxyl functionalities. These nanotubes were suspended in 5.0 mL of DMSO for further use.

2.4 Construction of the biosensor

First, 1.0 mL of a mixed solution consisting of 15 mM PPD and 5 mM PABA was added into 5.0 mL of 1 M HCl solution, followed by an intensive stirring in an ice/water bath at 350 rpm. Next, 4 mL of 5 mM sodium nitrite ($NaNO_2$) was further added into the above solution. After complete reaction for 10 min, the resultant mixture was transferred into an electrochemical cell to serve as the electrolyte solution. Then, three cycles of cyclic voltammetric scanning in the potential range from 0.5 to -0.4 V was applied to a gold electrode which had been pretreated to obtain a clean and mirror-like surface according to the conventional method.[37] This results in the electrochemical graft of the aryldiazo compounds onto the electrode surface successfully.

Meanwhile, 100 μL of the terminally carboxylated SWCNTs was mixed with equal volume of 50 mM pH 6.0 MES buffer containing 2 mg EDC and 2 mg NHS. After 30 min activation reaction at room temperature and centrifugation to remove the supernatants, the aryldiazonium salt-modified electrode prepared above was immersed into this activated SWCNT suspension to conduct a covalent linking reaction for 2 h. The resultant electrode was washed by 10 mM pH 7.4 Tris-HCl for three times and then blocked with a 2% BSA

solution for 60 min. Next, the electrode was further immersed into 100 μL of 40 mM oligo-PEG solution containing 2 mg EDC and 2 mg NHS to conduct another reaction for 60 min. After repeated washing by 10 mM pH 7.4 Tris-HCl, 3 μL of 5 μM Fc-DNA was applied to the electrode surface to conduct an assembly reaction at 37 °C for 60 min. Finally, the obtained electrochemical biosensor was carefully washed with 10 mM Tris-HCl buffer and stored at 4 °C for further use.

2.5 Assay procedure

The biosensor prepared above was first immersed into 40 μL of mixed solution consisting of different concentrations of miRNA-21 and 20 U of T7 Exo. It was then gently vortexed on a JN100-4 Heating & Cooling ThermoMixer (Jiminuo, Suzhou) to conduct an incubation reaction for 110 min at 25 °C. Next, the resultant electrode was repeatedly washed by 10 mM pH 7.4 Tris-HCl and then applied for the electrochemical measurement in 50 mM pH 7.4 Tris-HCl containing 0.1 M sodium perchlorate ($NaClO_4$). The electrochemical responses of the biosensor toward different concentrations of miRNA-21 were finally recorded by DPV in the potential scanning from 0.2 to 0.8 V and used for the quantitative analysis.

3. Results and discussion

3.1 Preparation of vertically aligned SWCNTs for the biosensor construction

Previous reports[38,39] have demonstrated that the diazonium salt couplings can achieve the simple covalent attachment of vertically aligned SWCNTs on electrode surfaces, and the assembly of SWCNTs on the tethered aryldiazonium layer can increase the electronic coupling between the electrode and outside environment. As a useful monolayer forming species, oligo-PEG is commonly used to adjust the assembly of various nanointerfaces and both resist the non-specific adsorption of biomolecules.[39,40] To obtain an orderly

View Article Online
DOI: 10.1039/C9NR02543J

arrangement of the vertically aligned SWCNTs on the electrode surface, this work adopts a mixed solution consisting of PPD and PABA to conduct the diazotization reaction. This reaction in a strong acid solution with the presence of $NaNO_2$ leads to the conversion of the above aromatic compounds into mixed aryldiazonium cations.[38] When the gold electrode was immersed into the resultant aryldiazonium salt solution to conduct the cyclic voltammetric scanning from 0.5 to -0.4 V, an obvious reduction peak corresponding to the electrochemical reduction of the aryldiazonium cations into radical deposition at the electrode[39] appears at about -0.18 V in the first cycle (not shown). During the second cycle, this reduction peak disappears completely and the cyclic voltammogram trends to steady with a small background current. This phenomenon indicates the successful formation of the mixed aryldiazonium salts with exposed amino and carboxyl groups onto the electrode surface. Then, by virtue of carbodiimide chemistry for the further covalent linking of the terminally carboxylated SWCNTs and the oligo-PGE molecules with amino termini, respectively, the vertically aligned SWCNT-modified electrode with space interval of oligo-PEG can be thus obtained.

As a powerful electrochemical technique to monitor the interfacial properties of electrodes, EIS was used to investigate the interfacial resistance change of the gold electrode during the above modification process (Fig. S1, ESI†). Compared with the bare electrode, its electrode modification by the aryldiazonium salts results in an obvious interfacial resistance increase. This result well confirms the successful diazotization at the electrode, which leads to the electron transfer prevention to the $Fe(CN)_6^{3-}/Fe(CN)_6^{4-}$ redox probe correspondingly.[38,39] After the covalently linking of SWCNTs onto the electrode surface further, the interfacial resistance of the resultant electrode decreases drastically. This phenomenon should be attributed to the outstanding electroconductivity of SWCNTs. It also demonstrates the successful immobilization of the terminally

View Article Online
DOI: 10.1039/C9NR02543J

carboxylated SWCNTs at the aryldiazonium salt-modified electrode.

AFM was further used to characterize the morphology change of the electrode surface upon its modification by diazonium salt and the covalent linking of SWCNTs in succession. As shown in Fig. 2, the electrode surface which was electrochemically grafted by the diazonium salt shows a layer of aggregations with homogeneous distribution. After further covalent linking of SWCNTs, a large number of neatly arranged vertical nanostructures appear on the electrode surface, and the average height of the vertically aligned "nano forest" is nearly 50 nm. This result indicates the successful chemical assembly of the vertically aligned SWCNTs on the electrode surface. Thus the formed "nano forest" structures of SWCNTs with good space interval of oligo-PEG can provide completely exposed sidewalls for the free noncovalent adsorption of Fc-DNA.[26,28] Compared with the XPS spectrum of the vertically aligned SWCNT-modified electrode, obvious Fe 2p peak at 707 eV, which should be corresponding to the Fc labels newly appears after its incubation in the Fc-DNA solution (Fig. 2C). This result demonstrates the successful binding of the Fc-DNA at the vertically aligned SWCNT-modified electrode to obtain the miRNA-21 biosensor.

Preferred position for Fig. 2

3.2 Electrochemical biosensing and signal amplification mechanisms

The constructed biosensor was then employed for the biorecognition of the target analyte of miRNA-21, and its electrochemical signal response was measured by DPV. As shown in Fig. 3a, the vertically aligned SWCNT-modified electrode is featureless in the potential scanning range from 0.2 to 0.8 V. After its incubation in an Fc-DNA solution, a well-defined oxidation peak clearly appears at about 0.56 V (Fig. 3b). This should be attributed to the excellent electrochemical behavior of the Fc labels. It further confirms the successful noncovalent adsorption of Fc-DNA onto the sidewalls of the vertically aligned

View Article Online
DOI: 10.1039/C9NR02543J

SWCNTs to obtain the biosensor. However, upon the further incubation of the biosensor into an analyte solution containing of 100 pM miRNA-21, the peak current of the biosensor decreases obviously (Fig. 3c). This result should ascribe to the successful biorecognition of the biosensor toward the miRNA target for nucleic acid hybridizations. As the formed Fc-DNA/miRNA-21 duplex cannot bind onto the surface of SWCNTs, the electrochemical signal of the biosensor decreases correspondingly.

In order to further improve this electrochemical signal decrease, this work introduces a useful nuclease of T7 Exo to achieve the highly efficient enzymatic cleavage for signal amplification. As T7 Exo can stepwisely catalyze the digestion of the single-stranded DNA in the DNA/RNA duplex from its 5' to 3' terminus,[6,41] once the Fc-DNA/miRNA-21 duplexes are produced from the biorecognition reactions and released into the detection solution, the enzymatic cleavage of T7 Exo will induce the release of the miRNA-21 target from these duplexes to participate the biorecognition reaction at the biosensor again. So this target recycling reaction will cause drastic release of Fc-DNA from the biosensor surface and thus achieve the great signal amplification of the biosensing method. From Fig. 3d one can find that the addition of 20 U of T7 Exo into the sample solution leads to significant reduce of the DPV peak current of the biosensor. It well demonstrates the feasibility of the T7 Exo-assisted target recycling based signal amplification strategy designed in this work. Hence, by combination of the highly efficient biorecognition reaction at the vertically aligned SWCNT-based biosensor and the simple and powerful T7 Exo-assisted target recycling for signal amplification, a novel electrochemical biosensing method can be thus developed for the ultrasensitive detection of miRNA-21.

Preferred position for Fig. 3

3.3 Experimental optimizations

To ensure the highly efficient biorecognition reaction of the biosensor, a mixed solution

View Article Online
DOI: 10.1039/C9NR02543J

consisting of PPD and PABA was employed for the diazotization at the electrode and thus adjusting the space arrangement of the vertically aligned SWCNTs. As the terminally carboxylated SWCNTs and oligo-PEG molecules can be covalently linked with the amino and carboxyl termini of the diazonium salts, respectively, the ratio of PPD to PABA in the diazotization at a total concentration of 20 mM was first optimized. As shown in Fig. 4, the electrochemical signal of the biosensor toward blank control first increases with the ratio of PPD to PABA from 1/3 to 3. However, too higher of PPD, e.g. 7 times the amounts of PPD to PABA causes some decrease of the electrochemical signal of the biosensor. Meanwhile, its electrochemical response toward the miRNA-21 target also decreases obviously. This phenomenon can be explained that the increasing amount of PPD used for diazotization can lead to increasing linking of SWCNTs for the noncovalent adsorption of Fc-DNA, and thus enhance the electrochemical signal of Fc at the biosensor. Due to the absence of enough oligo-PEG molecules for the space interval, however, too higher amount of PPD will result in the difficult formation of the orderly arranged nanostructures at the electrode. This will not only affect the complete exposure of the sidewalls of SWCNTs for the noncovalent adsorption of Fc-DNA but also decrease the contact chance of the miRNA-21 target with the biosensor for highly efficient biorecognition. As the ratio of the PPD to PABA at 3 can produce the best performance of the electrochemical biosensor, it is adopted as the optimum condition in this work.

Preferred position for Fig. 4

To ensure the saturated coverage of Fc-DNA on the sidewalls of SWCNTs, the amount of Fc-DNA used for the biosensor preparation was further optimized. As shown in Fig. S2 (ESI†), the DPV response of the biosensor first increases with the concentration of Fc-DNA when it is below 5 μM. However, too larger concentration of Fc-DNA over 5 μM leads to a plateau value of the electrochemical response. It indicates that 3 μL of 5 μM

View Article Online
DOI: 10.1039/C9NR02543J

Fc-DNA can realize its saturated noncovalent adsorption at the vertically aligned SWCNTs based electrode. Thus, it is used as the optimum amount for the biosensor construction.

To achieve the largest enzymatic cleavage of T7 Exo for inducing the target recycling signal amplification, the amount of T7 Exo added into the sample solution was then optimized. As shown in Fig. 5A, the electrochemical response of the biosensor toward 100 pM miRNA-21first increases with the dosage of T7 Exo in the range increasing from 4 to 20 U. When the amount of T7 Exo added into the sample solution is over 20 U, a steady value is obtained. It indicates that 20 U of T7 Exo can lead to the saturated enzymatic reaction for the target recycling signal amplification. Thus it is selected as the optimum amount in this work.

In addition, the one-step incubation time of the biosensor in the sample solution was also optimized. From Fig. 5B one can find that the DPV signal of the biosensor toward 100 pM miRNA-21 first decreases with the increasing incubation time from 30 to 110 min, and then trends to a steady value when it is over 110 min. This result indicates that 110 min vortexed reaction of the biosensor immersed into the sample reaction can achieve the complete biorecognition and T7 Exo-assisted target recycling reactions. Thus 110 min incubation reaction of the biosensor is used as the optimum condition in this work.

Preferred position for Fig. 5

3.4 Application for the electrochemical detection of miRNA-21

Under the optimum conditions, the electrochemical responses of the vertically aligned SWCNT-based biosensor toward the miRNA-21 target at different concentrations were investigated. From Fig. 6 one can find that the DPV peak currents of the biosensor decrease with the increase of the concentrations of the miRNA-21 target analyte. A good linear relationship is shown between the DPV responses and the logarithm values of

miRNA-21 concentrations in the range from 0.01 pM to 100 pM (R=0.996). The limit of detection (LOD) at a signal-to-noise ratio of 3 is estimated to be 3.5 fM. As shown in Table S1 (ESI†), this LOD value is lower than that previously reported in several miRNA biosensing methods.[10,11,15,19,34–36] This well confirms the excellent performance superiority of the vertically aligned SWCNTs and the T7 Exo-assisted target recycling on the sensitivity improvement of the miRNA-21 biosensor.

Preferred position for Fig. 6

Five vertically aligned SWCNT-based electrochemical biosensors were constructed with the same method and used for the repeated detection of the miRNA-21 target by using the developed signal transduction strategy. The relative standard deviations (RSDs) from five repeated measurements are 5.1% and 3.9% for the 0.1 and 10 pM of miRNA-21, respectively. When not in use, the biosensor was stored at 4 ^{o}C in dry. The experiments show that 96.1% of the initial electrochemical response of the biosensor toward 100 pM miRNA-21 can remain within one week's storage. These results indicate that the miRNA-21 biosensor has excellent reproducibility and stability.

To investigate the specificity of the biosensor, several other miRNAs such as miRNA-141 (miR-141), miRNA-155 (miR-155) and miRNA-199a (miR-199a) were used to replace miRNA-21 in the sample solution, respectively. By employment of the signal transduction strategy same to miRNA-21, their electrochemical signal responses were recorded. In comparison with the drastic electrochemical signal response of 100 pM miRNA-21 at the biosensor, 100 times the concentration of other miRNAs does not produce obvious electrochemical signal response over the blank control (Fig. 7). These results demonstrate that the miRNA-21 biosensor and the developed signal transduction strategy have excellent specificity and selectivity for practical applications.

Preferred position for Fig. 7

View Article Online
DOI: 10.1039/C9NR02543J

To further assess the reliability of the biosensor, the miRNA-21 levels in healthy human serums, which were first diluted 10 times by Tris-HCl, were analyzed by this method. As no miRNA-21 over the lowest detection level of the method was found in the real samples, different concentrations of miRNA-21 analyte were added to conduct the recovery experiments. As shown in Table S2 (ESI†), the recoveries are from 96.8 to 107% with RSD less than 5.1%. The result reveals that this biosensing method has satisfactory reliability and practicality for real sample analysis.

4. Conclusions

By combination of the vertically aligned SWCNT-based biosensor for the highly specific biorecognition with the T7 Exo-assisted target recycling for signal amplification, this work successfully develops a novel electrochemical bioassay method for miRNA-21 detection. The electrode modification by aryldiazonium salts enables the easy construction of the vertically aligned nanostructures of SWCNTs and also ensures the excellent chemical stability of the biosensors. The vertically aligned SWCNTs with good space interval by oligo-PEG enable their free adsorption of Fc-DNA for the successful construction of the biosensor and the highly efficient biorecognition of the biosensor toward miRNA-21 for sensitive signal transduction. The T7 Exo-assisted target recycling triggered by the one-step biorecognition reaction at the biosensor not only leads to a drastic increase of the signal/target ratio for signal amplification but also ensures convenient manipulations of the method. Meanwhile, this work does not involve expensive instruments, high analytical cost, inconvenient multi-step washing and separation as well as complicated DNA primer design and nanoprobe synthesis. Therefore, this vertically aligned SWCNT-based electrochemical biosensing method with excellent performance superiority possesses extensive application prospects in the clinical disease diagnosis field.

View Article Online
DOI: 10.1039/C9NR02543J

Conflicts of interest

There are no conflicts to declare.

Acknowledgements

This work was financially supported by the National Natural Science Foundation of China (21475033), Science and Technology Foundation for Excellent Creative Research Group of Hubei Provincial Department of Education, China (T201810), and Open Fund of Hubei Key Laboratory of Pollutant Analysis and Reuse Technology, China (PA20170207).

Notes and references

1 S. A. Byron, K. R. V. Keuren-Jensen, D. M. Engelthaler, J. D. Carpten and D. W. Craig, *Nat. Rev. Genet.*, 2016, **17**, 257–271.

2 H. Dong, J. Lei, L. Ding, Y. Wen, H. Ju and X. Zhang, *Chem. Rev.*, 2013, **113**, 6207–6233.

3 J. Li, P. Lei, S. Ding, Y. Zhang, J. Yang, Q. Cheng and Y. Yan, *Biosens. Bioelectron.*, 2016, **77**, 435–441.

4 R. Tavallaie, J. McCarroll, M. L. Grand, N. Ariotti, W. Schuhmann, E. Bakker, R. D. Tilley, D. B. Hibbert, M. Kavallaris and J. J. Gooding, *Nat. Nanotechnol.*, 2018, **13**, 1066–1071.

5 J. Zhang, L. L. Wang, M. F. Hou, Y. K. Xia, W. H. He, A. Yan, Y. P. Weng, L. P. Zeng and J. H. Chen, *Biosens. Bioelectron.*, 2018, **102**, 33–40.

6 P. Miao, T. Zhang, J. Xu and Y. Tang, *Anal. Chem.*, 2018, **90**, 11154−11160.

7 X. Zhang, Z. Yang, Y. Chang, M. Qing, R. Yuan and Y. Chai, *Anal. Chem.*, 2018, **90**, 9538–9544.

8 J. Dong, G. Chen, W. Wang, X. Huang, H. Peng, Q. Pu, F. Du, X. Cui, Y. Deng and Z. Tang, *Anal. Chem.*, 2018, **90**, 7107–7111.

9 J. Lee, Y. K. Kim, S. Lee, S. Yoon and W. K. Kim, *Sens. Actuators B*, 2019, **282**, 861–867.

10 B. Z. Chi, R. P. Liang, W. B. Qiu, Y. H. Yuan and J. D. Qiu, *Biosens. Bioelectron.*, 2017, **87**, 216–221.

11 J. Zhou, Z. Li, M. Ying, M. Liu, X. Wang, X. Wang, L. Cao, H. Zhang and G. Xu, *Nanoscale*, 2018, **10**, 5060–5064.

12 L. Peng, Y. Yuan, X. Fu, A. Fu, P. Zhang, Y. Chai, X. Gan and R. Yuan, *Anal. Chem.*, 2019, **91**, 3239–3245.

13 P. Zhang, Z. Li, H. Wang, Y. Zhuo, R. Yuan and Y. Chai, *Nanoscale*, 2017, **9**, 2310–2316.

14 T. Hou, N. Xu, W. Wang, L. Ge and F. Li, *Anal. Chem.*, 2018, **90**, 9591–9597.

15 S. Liu, H. Cao, X. Wang, W. Tu and Z. Dai, *Nanoscale*, 2018, **10**, 16474–16478.

16 A. A. Jamali, M. Pourhassan-Moghaddam, J. E. N. Dolatabadi and Y. Omidi, *TrAC-Trend. Anal. Chem.*, 2014, **55**, 24–42.

17 Y. X. Chen, K. J. Huang and K. X. Niu, *Biosens. Bioelectron.*, 2018, 99, 612–624.

18 Q. Tian, Y. Wang, R. Deng, L. Lin, Y. Liu and J. Li, *Nanoscale*, 2015, **7**, 987–993.

19 D. Zhu, W. Liu, D. Zhao, Q. Hao, J. Li, J. Huang, J. Shi, J. Chao, S. Su and L. Wang, *ACS Appl. Mater. Interfaces*., 2017, **9**, 35597–35603.

20 L. Zhu, L. Luo and Z. Wang, *Biosens. Bioelectron.*, 2012, **35**, 507–511.

21 F. Li, J. Peng, J. Wang, H. Tang, L. Tan, Q. Xie and S. Yao, *Biosens. Bioelectron.*, 2014, **54**, 158–164.

22 H. Ju, *App. Mater. Today*, 2018, **10**, 51–71.

23 X. Meng, K. Zhang, W. Dai, Y. Cao, F. Yang, H. Dong and X. Zhang, *Chem. Sci.*, 2018, **9**, 7419–7425.

24 T. Hu, L. Zhang, W. Wen, X. Zhang and S. Wang, *Biosens. Bioelectron.*, 2016, **77**, 451–456.

25 Z. Wang and Z. Dai, *Nanoscale*, 2015, **7**, 6420–6431.

26 R. Yang, Z. Tang, J. Yan, H. Kang, Y. Kim, Z. Zhu and W. Tan, *Anal. Chem.*, 2008, **80**, 7408–7413.

27 F. Patolsky, Y. Weizmann and I. Willner, *Angewan. Chem.*, 2004, **116**, 2165–2169.

28 F. J. Rawson, C. L. Yeung, S. K. Jackson and P. M. Mendes, *Nano Lett.*, 2013, **13**, 1–8.

29 M. Pumera, *Chem. Eur. J.*, 2009, **15**, 4970–4978.

30 M. Yan, W. Bai, C. Zhu, Y. Huang, J. Yan and A. Chen, *Biosens. Bioelectron.*, 2016, **77**, 613–623.

31 J. Dai, H. He, Z. Duan, Y. Guo and D. Xiao, *Anal. Chem.*, 2017, **89**, 11971–11975.

32 Z. Wu, H. Fan, N. S. R. Satyavolu, W. Wang, R. Lake, J. H. Jiang and Y. Lu, *Angew. Chem. Int. Ed.*, 2017, **56**, 8721–8725.

33 H. Xie, Y. Chai, Y. Yuan and R. Yuan, *Chem. Commun.*, 2017, **53**, 8368–8371.

34 H. Wu, Y. Liu, H. Wang, J. Wu, F. Zhu and P. Zou, *Biosens. Bioelectron.*, 2016, **81**, 303–308.

35 L. Zhang, G. Zhu and C. Zhang, *Anal. Chem.*, 2014, **86**, 6703–6709.

36 Y. Yu, Z. Chen, L. Shi, F. Yang, J. Pan, B. Zhang and D. Sun, *Anal. Chem.*, 2014, **86**, 8200–8205.

37 H. Cheng, L. Xu, H. Zhang, A. Yu and G. Lai, *Analyst*, 2016, **141**, 4381–4387.

38 G. Liu, S. Wang, J. Liu and D. Song, *Anal. Chem.*, 2012, **84**, 3921–3928.

39 W. Guo, F. Jiang, J. Chu, D. Song and G. Liu, *J. Electroanal. Chem.*, 2013, **703**, 63–69.

40 C. Cao, Y. Zhang, C. Jiang, M. Qi and G. Liu, *ACS Appl. Mater. Interfaces*, 2017, **9**, 5031–5049.

41 T. Hou, N. Xu, W. Wang, L. Ge and F. Li, *Anal. Chem.*, 2018, **90**, 9591–9597.

View Article Online
DOI: 10.1039/C9NR02543J

Figure captions:

Fig. 1 Schematic illustration of the preparation process of the vertically aligned SWCNT-modified electrode (A) and the miRNA-21 biosensor along with its electrochemical signal transduction principle (B).

Fig. 2 AFM images of the aryldiazonium salt (A) and vertically aligned SWCNTs (B) modified electrodes; and (C) the XPS spectra of the vertically aligned SWCNT-modified electrode (a) and the as-prepared miRNA-21 biosensor (b).

Fig. 3 DPV responses of the vertically aligned SWCNT-modified electrode (a) and the as-prepared electrochemical biosensor (b, c, d) in 50 mM pH 7.4 Tris-HCl containing 0.1 M $NaClO_4$ before (b) and after (c, d) incubation of 100 pM miRNA-21 in absence (c) and presence (d) of 20 U of T7 Exo.

Fig. 4 DPV responses of the biosensors prepared from the electrode modification with the mixed aryldiazonium salt solutions at different ratios of PPD to PABA, toward blank control (in grey) and 100 pM miRNA-21 (in red).

Fig. 5 Effects of the volume of T7 Exo at 2 U μL^{-1} used for enzymatic cleavage (A) and the one-step incubation time (B) on the DPV responses of 100 pM miRNA-21.

Fig. 6 DPV responses of different concentrations of miRNA-21 at the biosensor and the calibration plot of the method (the inset). From bottom to top, the concentrations of miRNA-21 correspond to 0, 0.01 pM, 0.1 pM, 1 pM, 10 pM, 100 pM and 1 nM.

Fig. 7 DPV responses of the electrochemical biosensor toward blank control, 10 nM of miR-141, miR-155 and miR-199a as well as 100 pM of miRNA-21.

Figure 1

View Article Online
DOI: 10.1039/C9NR02543J

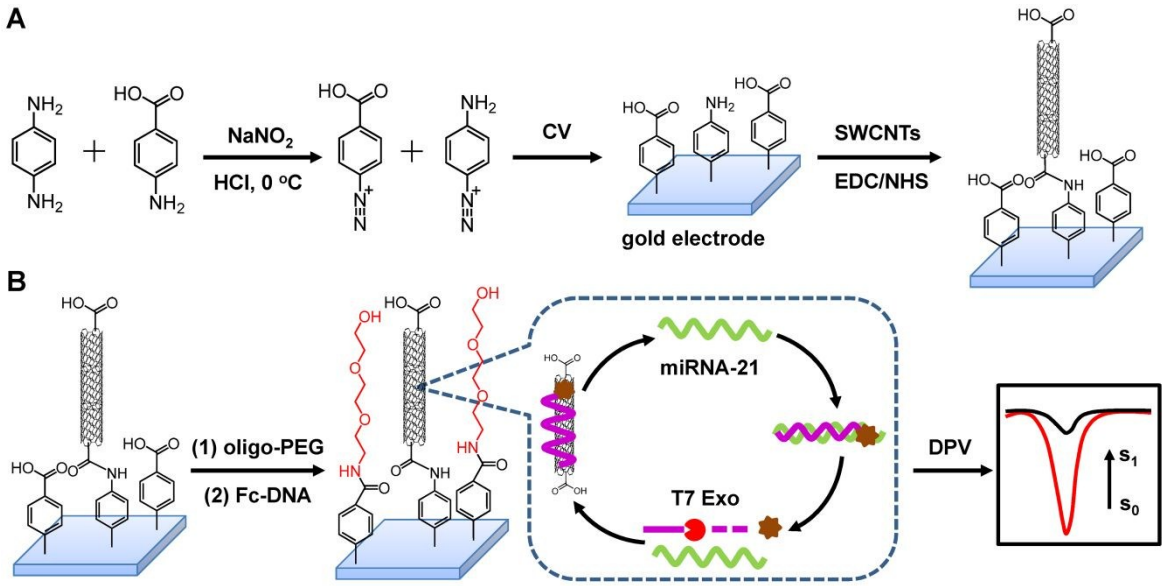

Figure 2

View Article Online
DOI: 10.1039/C9NR02543J

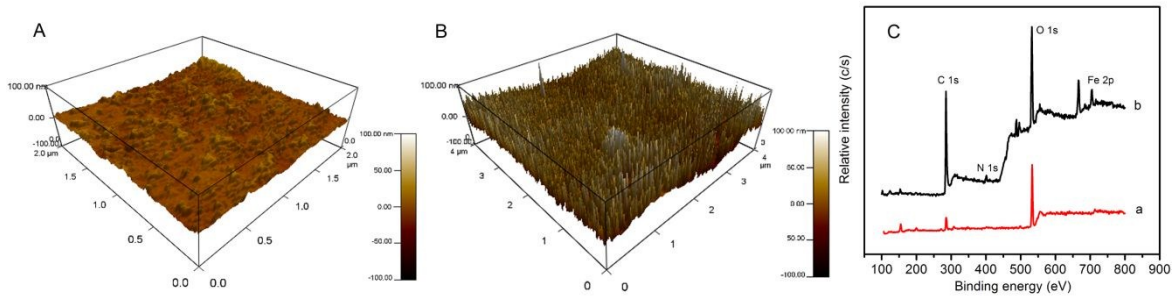

Figure 3

View Article Online
DOI: 10.1039/C9NR02543J

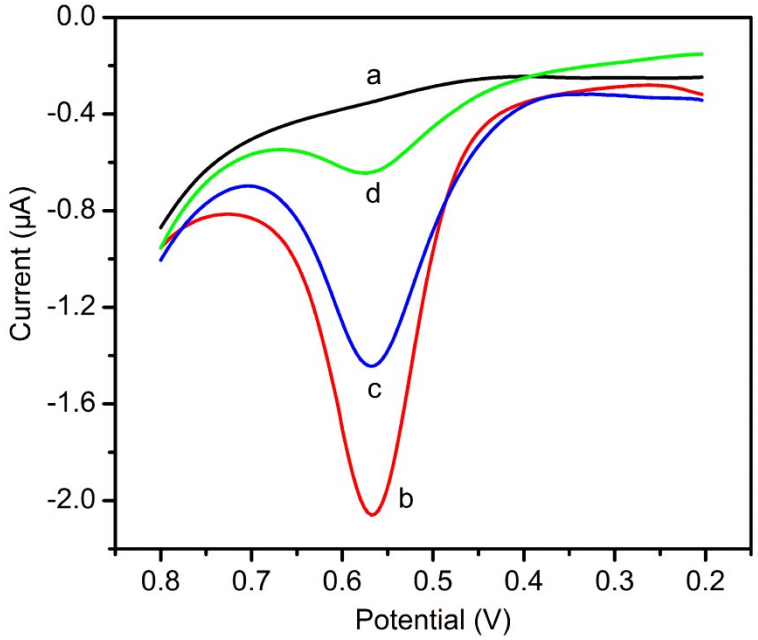

Figure 4

View Article Online
DOI: 10.1039/C9NR02543J

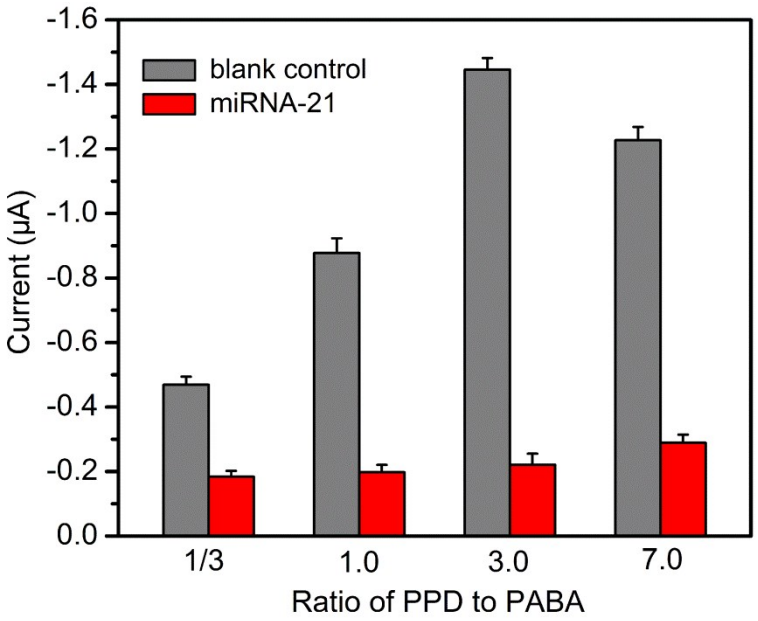

Figure 5

View Article Online
DOI: 10.1039/C9NR02543J

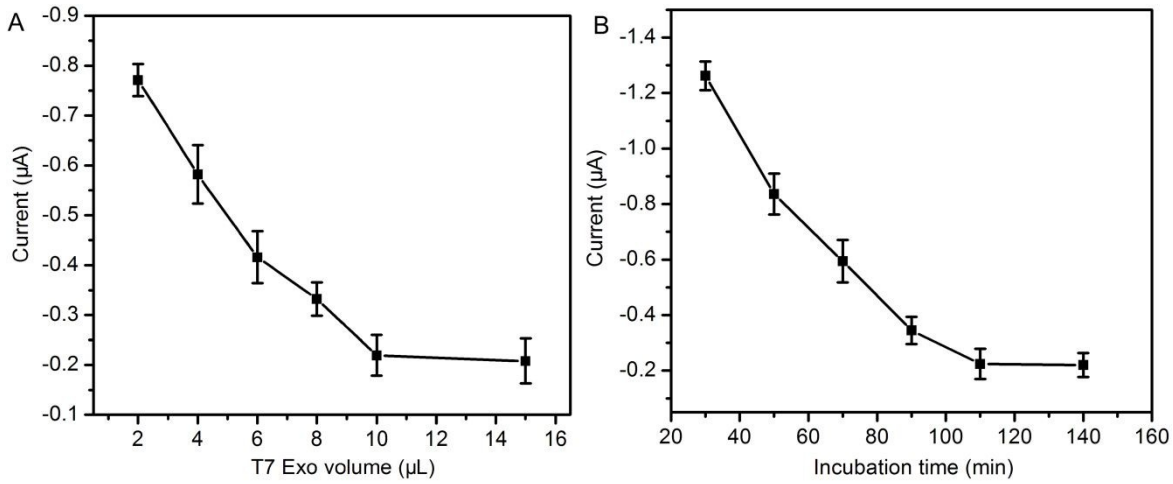

Figure 6

View Article Online
DOI: 10.1039/C9NR02543J

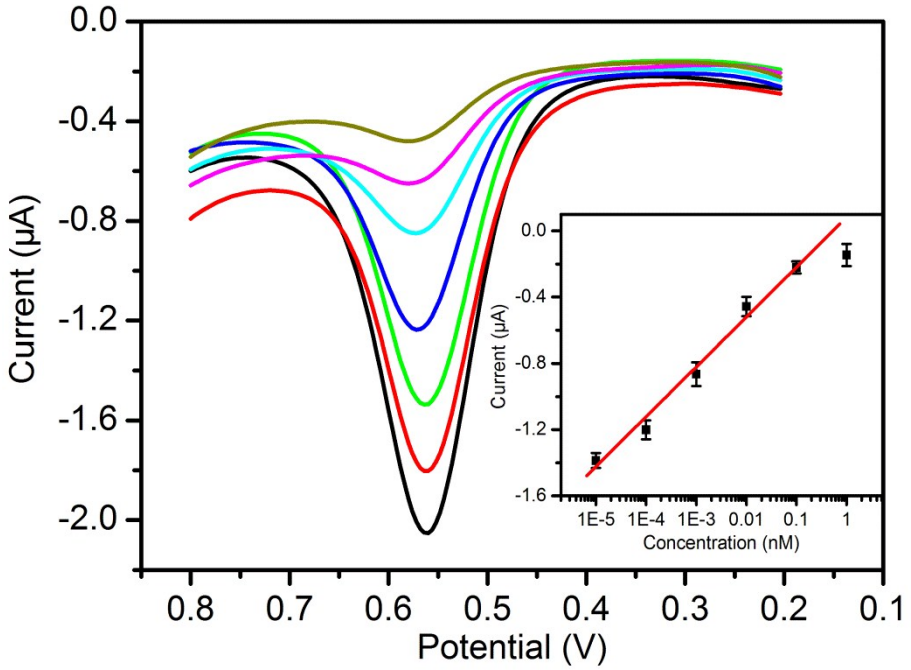

Figure 7

View Article Online
DOI: 10.1039/C9NR02543J

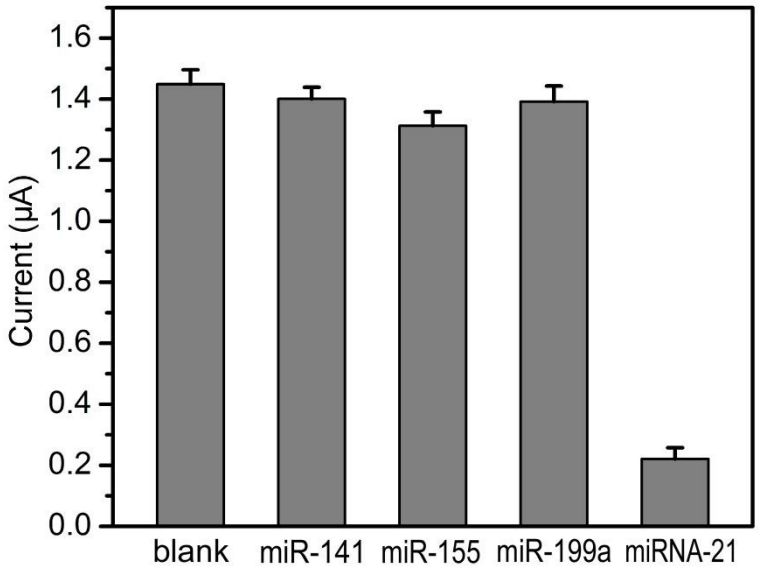

View Article Online
DOI: 10.1039/C9NR02543J

Graphical abstract

The one-step biorecognition at a vertically aligned SWCNT-based biosensor and T7 exonuclease-assisted target recycling enable the ultrasensitive bioassay of microRNA-21.